CHALMERS

DRAFT November 19, 2012

TITLE OF PROJECT

Thesis for the degree of Master of Science

ANDREAS BÜLLING

Department of Mathematical Sciences
CHALMERS UNIVERSITY OF TECHNOLOGY
Gothenburg, Sweden 2012
Master's Thesis 2012:1

Abstract

Lorem ipsum dolor sit amet, consectetur adipisicing elit, sed do eiusmod tempor incididunt ut labore et dolore magna aliqua. Ut enim ad minim veniam, quis nostrud exercitation ullamco laboris nisi ut aliquip ex ea commodo consequat. Duis aute irure dolor in reprehenderit in voluptate velit esse cillum dolore eu fugiat nulla pariatur. Excepteur sint occaecat cupidatat non proident, sunt in culpa qui officia deserunt mollit anim id est laborum.

Acknowledgements

Lorem ipsum dolor sit amet, consectetur adipisicing elit, sed do eiusmod tempor incididunt ut labore et dolore magna aliqua. Ut enim ad minim veniam, quis nostrud exercitation ullamco laboris nisi ut aliquip ex ea commodo consequat. Duis aute irure dolor in reprehenderit in voluptate velit esse cillum dolore eu fugiat nulla pariatur. Excepteur sint occaecat cupidatat non proident, sunt in culpa qui officia deserunt mollit anim id est laborum.

The Authors, Location 11/9/11

Contents

1

Introduction

Short intro for this section

1.1 Background

Historically - LBM and modelling of electrohydrodynamics. Development til today.

1.2 General problem description

Description of problem + what we want to achieve in this work.

1.3 Outline

How is this report structured?

2

Electrohydrodynamics in microchannels

In this chapter, the fundamental physics behind electrokinetic flow, important for later discussions, will be presented. Particularly, a modelling approach based on the coupling of Navier-Stokes, Nernst-Planck and Poission's equations is given.

2.1 Basic concepts of electrokinetic flow

Electrohydrodynamics involves the study of electric phenomena on fluid flow. How fluids carrying electrical charges (electrolytes) react upon external electrical fields or interact with charged objects are examples of problems that arise in this field.

2.1.1 Electrical double layers

As a charged object is brought into contact with an electrolyte it is, qualitatively, easily deduced that ions with a sign of charge opposite to that of the object will be attracted to the object and ions with the same sign of charge will be repelled. These two distinct categories of ions will from hereon be referred to as counter- and co-ions respectively. In this case, for a neutral electrolyte, a surplus of counter-ions will be present in the direct vicinity of the object and a surplus of co-ions will be present at some other location further from the object.

The area with a surplus of counter-ions in an electrolyte in contact with a charged object is often referred to as an electrical double layer. Two distinct regions will be formed in this area, thus the name double layer. The two layers are often referred to as the Stern layer (adsorbed ions) and the diffusive layer (mobile ions). The Stern layer is usually several orders of magnitude thinner than the diffusive layer and is therefore seldom considered when it comes to modelling [**?**].

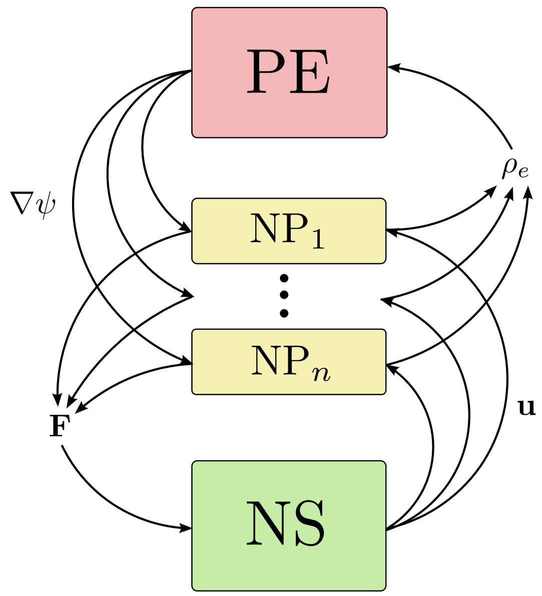

Figure 2.1: Visualisation of the coupling between the three equations present in the model. Poisson's equation (PE), The set of Nernst-Planck equations (NP_1 ... NP_n) and the Navier-Stokes equations (NS). The dependencies have also be marked with arrows indicating what quantities for a certain equation that are needed from an other.

2.1.2 Electroosmosis

As fluid carrying a net charge, e.g. in the diffusive layer of an EDL, is under influence of an electric field, the charged particles will move due to the electric forces. As the charge particles move, they will affect the surrounding liquid, causing it move as well. This liquid motion is often referred to as electroosmotic flow. [**?**]

2.2 Complete physical model

To model the fluid motion of a charged fluid under influences of electrostatic forces, a coupling between different models is considered.

The electric field and potential in the system are obtained from solving Poisson's equation for electrostatics (section 2.3) with a given charge density. This Charge density is obtained from the Nernst-Planck equation (section 2.4) by including effects on the charge distribution from the electric field previously mentioned, diffusion and advection. The advective charge flux is given from the velocity field in the fluid that is obtatined by solving the Navier-Stokes equations (section 2.5). Forces due to present electric fields on net charged areas of the fluid also couples the NS equations to the NP equation. More about the force coupling is discussed in sections. 2.6 and 2.7. The coupling between the different equations are visualised in fig. 2.1.

2.3 The potential - Poisson's equation

To be able to model the flow dynamics of liquids in a channel with present EDLs, the potential and charge distribution in the channel must be determined. These quantities are mutually related through Poisson's equation for electrostatics:

$$\nabla^2 \psi = -\frac{\rho_e}{\epsilon_r \epsilon_0} \tag{2.1}$$

where ψ is the electrical potential, ρ_e the electrical charge density, ϵ_r is the relative permittivity and ϵ_0 the vacuum permittivity. Under certain assumptions, the charge density may be explicitly determined as a function of the potential distribution, one such result is the so called Poisson-Boltzmann equation, further discussed in section 2.4.2.

2.3.1 Boundary conditions

At the charged boundaries, most physical situations may be covered by either specifying the potential or the surface charge density. The former would be a boundary condition of Dirichlet type:

$$\psi(\mathbf{x}) = \zeta(\mathbf{x}) \ , \ \ \mathbf{x} \in \Gamma \tag{2.2}$$

and the latter a boundary condition of Neumann type:

$$\nabla \psi(\mathbf{x}) \cdot \mathbf{n} = -\frac{\sigma(\mathbf{x})}{\epsilon_0 \epsilon_r} \ , \ \ \mathbf{x} \in \Gamma \tag{2.3}$$

where Γ denotes the boundary of the domain and $\mathbf{n}$ is the normal to the boundary surface. [**?**]

2.4 The transport of charges - Nernst-Planck equation

The charge concentration in an electrolyte is indeed affected by its environment. In the model proposed here, influences from: advection of the electrolyte, diffusion due to concentration gradients and effects from the electric field originating from charged objects placed at the border or in the flow is considered. Charge conservation without any external sources of the ion density, $\mathrm{C}(\mathbf{x}, t)$, gives:

$$\frac{\partial \mathrm{c}}{\partial t} + \nabla \cdot \mathbf{J} = 0 \tag{2.4}$$

where $\mathbf{J}(\mathbf{x}, \mathrm{t})$ is the net flux induced by the effects described above. Explicit expressions for the fluxes due to advection and diffusion respectively are

$$\mathbf{J}_{adv} = \mathrm{c}\mathbf{u} \tag{2.5}$$

and

$$\mathbf{J}_{dif} = -D\nabla \mathrm{C} \tag{2.6}$$

where $\mathbf{u}$ is the advective velocity and D is a diffusion coefficient. The ionic flux due to the presence of an electric potential, $\psi(\mathbf{x}, t)$, is given by the Nernst equation [**?**]:

$$\mathbf{J}_{ele} = -\frac{zq_e D}{k_B T}\mathrm{c}\nabla\psi \tag{2.7}$$

where z is the relative charge of an ion, q_e is the fundamental charge, k_B is the Boltzmann constant and T is the temperature of the fluid.

Summing up the fluxes and putting them into eq. (2.4) gives

$$\frac{\partial \mathrm{c}}{\partial t} = \nabla \cdot \left[D\nabla \mathrm{C} - \mathrm{c}\mathbf{u} + \frac{zq_e D}{k_B T}\mathrm{c}\nabla\psi \right] \tag{2.8}$$

which is a known result often referred to as the Nernst-Planck equation. The advective velocity, $\mathbf{u}$, and the potential gradient, $\nabla\psi$, are obtained from couplings to the Navier-Stokes and Poisson's equation respectively. More about the coupling between the equations is discussed in section 2.2.

2.4.1 Boundary conditions

Depending on the physical situation that is being modelled, different conditions may be imposed at the boundaries of the domain. Throughout this work, at hard boundaries (walls), the charge flux through the boundary is set to zero, i.e.:

$$\mathbf{J} \cdot \mathbf{n} = 0 \,, \ \ \mathbf{x} \in \Gamma \tag{2.9}$$

where $\mathbf{n}$ denotes the normal to the surface and Γ is the boundary of the domain.

2.4.2 Poisson-Boltzmann equation

Consider a system consisting of an electrolyte in contact with a (flat) charged wall. Under certain assumptions, it is possible to explicitly determine the charge density in eq. (**??**) as a function of the electric potential. E.g. if there is no advection present and if the system has reached a steady state, i.e. $\partial c/\partial t = 0$ and $\mathbf{u} = \mathbf{0}$ we have:

$$D\nabla \mathrm{C} + \frac{zq_e D}{k_B T}\mathrm{c}\nabla\psi = \alpha \tag{2.10}$$

where α is some arbitrary constant. Due to the steady state assumption, what the equation above actually says is that the net flux of charge in the system is constant. Since no flux of charge is wanted to flow through the wall boundary, the flux is set to zero on the wall and since the flux is constant it will therefore be zero everywhere in the liquid, i.e. $\alpha = 0$.

Considering only a one-dimensional situation with a position variable y varying in a direction out from the wall into the liquid, eq. (2.10) reads

$$\frac{1}{\mathrm{c}}\frac{d\mathrm{c}}{dy} + \frac{zq_e}{k_BT}\frac{d\psi}{dy} = 0. \tag{2.11}$$

The charge density is determined by solving eq. (2.11) for c, i.e. integrating the equation. In order to avoid introducing additional unknown quantities, the equation is integrated to far away from the wall where the potential from the EDL is assumed to have decreased to zero and where the concentrations, c^{∞}, of the electrolyte is known.

$$\int_y^{\infty} d\ln(\mathrm{c}(y')) = -\frac{zq_e}{k_BT}\int_y^{\infty} d\psi(y') \tag{2.12}$$

This gives an expression for $C(y)$:

$$\mathrm{c}(y) = \mathrm{c}^{\infty}\exp\left(-\frac{zq_e\psi(y)}{k_BT}\right). \tag{2.13}$$

In a general case, there may be several species of ions in the electrolyte, the net charge density, ρ_e, is then given by simply summing up the contributions from the different species:

$$\rho_e = q_e\sum_i z_i\mathrm{c}_i. \tag{2.14}$$

Summarising eqs. (2.1), (2.13) and (2.14) gives the Poisson-Boltzmann equation in one dimension

$$\frac{d^2\psi(y)}{dy^2} = -\frac{q_e}{\epsilon_r\epsilon_0}\sum_i z_i\mathrm{c}_i^{\infty}\exp\left(-\frac{z_iq_e\psi(y)}{k_BT}\right). \tag{2.15}$$

The Debye–Hückel approximation

Historically, the non-linear nature of eq. (2.15) complicated when it came to solving it. This was a major difficulty in the past when the computational power at hands were rather limited. A linearisation is therefore sometimes done, this linear version of the PB equation is often referred to as the Debye–Hückel approximation. The solution of the linearisation gives however, something to compare with and will be used when defining a characteristic length scale of the EDL.

For a 1:1 electrolyte solution, eq. (2.15) reduces to

$$\frac{d^2\psi(x)}{dx^2} = \frac{2n^{\infty}q_ez}{\epsilon_r\epsilon_0}\sinh\left(\frac{zq_e\psi(x)}{k_BT}\right). \tag{2.16}$$

and the linearised equation is

$$\frac{d^2\psi(x)}{dx^2} = \frac{2n^{\infty}q_e^2z^2}{\epsilon_r\epsilon_0k_BT}\psi(x) = \kappa^2\psi(x) \tag{2.17}$$

where κ^{-1} is the Debye length and gives a measure for the characteristic size of the EDL.

Limitations of the Poisson-Boltzmann model

As the Poisson-Boltzmann equation is derived several assumptions are made. First, the net flux of ions are assumed to be zero and that the advective contribution the flux is negligible. Thus, the PB equation is only applicable when the system is at (or very close) thermodynamical equilibrium.

TODO: Continue this discussion...

2.5 The velocity field - Navier-Stokes equations

In hydrodynamics, the Navier-Stokes equations are one of the most fundamental corner stones. They describe the motion of a fluid under the influence of various internal and external forces.

For later convenience and for reference when it comes to deriving the Lattice-Boltzmann formulation of the NS equation, a brief sketch of a derivation will here be presented. A most general form of the Navier-Stokes equation follows from momentum conservation

$$\frac{\partial(\rho\mathbf{u})}{\partial t} + \nabla\cdot(\rho\mathbf{u}\otimes\mathbf{u}) + \mathbf{Q} = 0 \tag{2.18}$$

where, ρ is fluid density, $\mathbf{u}$ is velocity and $\mathbf{Q}$ is a momentum source term (force per volume). Expanding the time derivative and the divergence terms respectively gives

$$\mathbf{u}\left(\frac{\partial\rho}{\partial t} + \nabla\cdot(\rho\mathbf{u})\right) + \rho\left(\frac{\partial\mathbf{u}}{\partial t} + \mathbf{u}\cdot\nabla\mathbf{u}\right) + \mathbf{Q} = 0. \tag{2.19}$$

By assuring mass conservation (without sources) we have that

$$\frac{\partial\rho}{\partial t} + \nabla\cdot(\rho\mathbf{u}) = 0 \tag{2.20}$$

and eq. (2.19) reduces to

$$\rho\left(\frac{\partial\mathbf{u}}{\partial t} + \mathbf{u}\cdot\nabla\mathbf{u}\right) + \mathbf{Q} = 0 \tag{2.21}$$

which together with eq. (2.20) is a general formulation of the Navier stokes equations.

The force term $\mathbf{Q}$, is determined by the physical properties of the fluid and from its environment. In this work, only incompressible Newtonian fluids will be studied. The force contribution to $\mathbf{Q}$ involved in that case is limited to viscous forces, pressure gradients in the fluid and to external force fields. Putting that into eqs. (2.20) and (2.21) gives

$$\nabla\cdot\mathbf{u} = 0 \tag{2.22}$$

and

$$\rho\left(\frac{\partial \mathbf{u}}{\partial t}+\mathbf{u}\cdot\nabla\mathbf{u}\right)=-\nabla \mathrm{P}+\mu\nabla^2\mathbf{u}+\mathbf{F} \tag{2.23}$$

where P is the pressure, μ the kinematic viscosity and $\mathbf{F}$ is the contributions from external forces.

2.5.1 Boundary conditions

At hard boundaries (walls), the boundary conditions to eqs. (2.22) and (2.23) are set on the velocity of either a Dirichlet or Neumann type. In most physical situations the Dirichlet condition is used which corresponds to that there is a friction between the fluid and the wall, usually full friction, i.e. when no relative movement between fluid and wall is present and the velocity at the wall boundary is set to zero, i.e.

$$\mathbf{u}=0\ ,\ \ \mathbf{x}\in\Gamma \tag{2.24}$$

where Γ denotes the boundary. The Neumann type conditions are used for no-friction walls where the normal component of the derivative of the velocity is specified, usually to zero.

At wet boundaries, inlets and outlets, of the domain various boundary conditions may be set. For instance the pressure or the velocity could be fixed. In the case of a fixed pressure boundary, a flow direction must also be specified for completeness. [**?**]

2.6 Pressure-driven electrokinetic flow

As a charged fluid is driven by a pressure gradient, a movement of charges, i.e. an electrical current will be induced. Due to the charge flux, a potential gradient will build up along the flow direction. This potential is usually referred to as the streaming potential, $\phi(\mathbf{x})$, and its magnitude is determined from the induced current through Ohm's law

$$\mathbf{J}=-\sigma\nabla\phi \tag{2.25}$$

where σ is the conductivity of the fluid. For a perfectly conducting fluid, no potential difference will be built up. Also a complete neutral solution will carry no net current and therefore will no potential difference build up in that case either.

Charges under the influence of an electric field will be affected by a force. Charges moving due to this force will, in a liquid, also pull liquid (uncharged) molecules with them. In a macroscopic limit, the force density affecting the charges in the liquid is assumed to affect the liquid as whole. The volumetric force affecting the fluid from the presence of the streaming potential is then given by:

$$\mathbf{F}=-\rho_e\nabla\phi \tag{2.26}$$

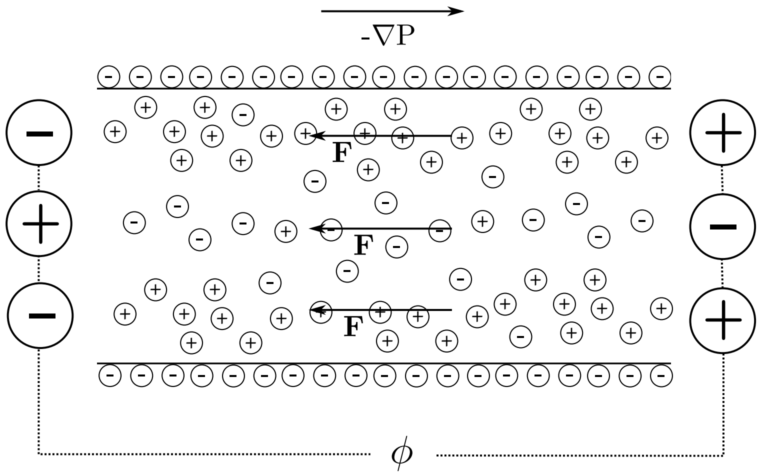

Figure 2.2: Example of an electroviscous system. The fluid is driven by a pressure gradient, ∇P. The direction of the forces on the fluid. The force originates from the potential difference that builds up along the channel, ϕ. The force is always opposite to the flow direction, thus slowing the flow down.

where ρ_e is the charge density. This is an example of how the charge density from the Nernst-Planck equation may couple to the force term in Navier-Stokes equations.

This force will always be affecting the fluid in an direction opposite of that of the net flux of charge, i.e. the force will slow the fluid down, this is illustrated in fig. 2.2. This effect that a moving net charged fluid is slowed down is called the *electroviscous effect*. The name originates from that a similar effect might be achieved by increasing the viscosity of the fluid.

2.7 Electroosmotic flow

Instead of driving the fluid flow through a pressure drop, a net charged fluid may be driven by an external electric field. This may be seen as the opposite case to that in section 2.6 where a current is induced by a pressure drop.

The volumetric force on the fluid from the external field, $\mathbf{E}_{ext}$, is given by

$$\mathbf{F} = \rho_e \mathbf{E}_{ext} \tag{2.27}$$

where ρ_e is the charge density. If the electric field is constant (or at least has the same direction) everywhere, the sign of the force is not in the same direction for a net charged positive area of the fluid as for a net charged negative. Thus the fluid may be either slowed down or sped up. This is a qualitative difference to pressure driven situation and is illustrated in fig. 2.3.

The electroviscous effect is in the case of pure electroosmotic flow usually neglected

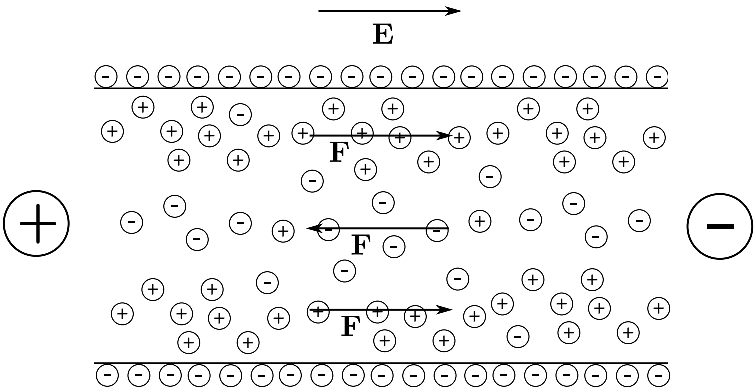

Figure 2.3: Example of an electroosmotic system. The fluid is driven by an external electric field, **E**. The direction of the forces on the fluid from the electric field is indicated with arrows. Note however that the fluid does not necessarily has to flow in the direction of the force, this due to viscous effects in the fluid.

as the field due to the streaming potential is, in most physical cases, small in comparison to the applied external field. [**?**]

3

The lattice-Boltzmann method

Rather than modelling on a macroscopic or microscopic scale, the lattice-Boltzmann method operates at a scale in between those, often referred to as a mesoscopic scale.

short intro of this section micro macro meso... new method..

3.1 Historical overview

With the introduction of electronic calculating machines came also a new possibility of tackling problems. New fields of computational science was born and methods for solving both new traditional problems were developed.

The idea of using a discrete and simplified version of the Boltzmann-equation dates back to the mid 60's [**?**] with an experimental attempt to model simple gas dynamics. However, at the time, this kind of statistical computational approaches was not considered a serious alternative for the modelling of more sophisticated fluid behaviour. It was first in the mid 80's when Frisch, Hasslacher and Pomeau showed that a lattice automaton, with a lattice of certain symmetry and that conserved mass and momentum in the collisions, reproduced the Navier-Stokes equations in a macroscopic limit. It was with this paper and the always increasing computational power that made the idea of fluid modelling on a mesoscopic scale a serious research topic.

The lattice gas automata (LGA) approach suffered from some flaws, e.g. that the boolean nature of the method introduced statistical noise and that lack of symmetry in the lattice made the advection non-isotropic. The statistical noise was usually dealt with by averaging which resulted in a coarsed domain and the advection issue was handled by introducing lattices of higher symmetry. As the flaws of the LGA approach was dealt with one after one, the method evolved into what we today know as the lattice-Boltzmann method, with the crucial refinement of using continuous distributions over boolean variables. [**?**]

3.2 The Boltzmann transport equation

The continuous lbe is bte.. distribution function

3.3 Basic idea of the LBM

As previously noted, the lattice-Boltzmann is a mesoscopic method. This means that the modelling is neither done on a molecular level nor by direct solving the macroscopic equations involved. The aim, in the most situations with the lattice-Boltzmann is indeed to solve some macroscopic equation but not direct. Instead a statistical model is used with various mesoscopic variables that, in some limit, reproduces the macroscopic variables. It is also possible to ensure that these variables fulfil a certain macroscopic equation by using a certain scheme.

Basically the lattice-Boltzmann method solves a discretised version of eq. (**??**) for the distribution functions and then macroscopic quantities are determined from the distribution functions. Both the spatial positions and the velocity space is discretised allowing the distributions to "sit" only at certain positions and to stream to neighbouring locations only in the directions specified by the discretised velocity space. Usually in two dimensions the velocity space is discretised into 9 distinct velocities, more about the choice of lattice is discussed in section 3.5. In this case 9 distribution functions are needed per node which might correspond to one or two macroscopic variables but is indeed fewer than the number of variables needed for a microscopic approach.

The discretised Boltzmann equation is referred to as the lattice-Boltzmann equation and is one of the fundamental corner stones in the lattice-Boltzmann method, it reads:

$$f_i(\mathbf{x} + \mathbf{c}_i\delta_t, t + \delta_t) - f_i(\mathbf{x}, t) = \Omega_i(\mathbf{x}, t) \tag{3.1}$$

where f_i denotes the distribution function for direction $\mathbf{c}_i$, δ_t is the time step and Ω_i is the (for now non-specified) collision operator. Various forms of collision operators exist and will be further discussed in section 3.4.

3.3.1 Computational algorithm

When solving eq. (3.1) two computational tasks is unidentified. Thus

3.4 The collision operator

discussions on different col. operators, focus on BGK since that is the one used. collision invariants..

3.4.1 The BGK operator

$$\Omega_i = -\omega \left[f_i(\mathbf{x}, t) - f_i^{(eq)}(\mathbf{x}, t) \right] \tag{3.2}$$

3.5 The lattice

symmetry... multi speed... weights ... D2Q9

$$w_i = ... \tag{3.3}$$

3.6 Asymptotic analysis

Methods from asymptotic analysis will, in this section, be used to investigate the macroscopic limit of the general LBE. Detailed and specific analyses for the three different equations considered will be presented in sections **??**, **??** and **??**. Asymptotic analysis is basically about describing mathematical objects in some limit, e.g. how a function behaves for large or small values of some parameter. Consider for example the series expansion of $\exp(\epsilon)$:

$$\exp(\epsilon) = 1 + \epsilon + \epsilon^2/2 + \epsilon^3/6 + \mathcal{O}(\epsilon^4) \tag{3.4}$$

It is clear that for sufficiently small values of ϵ, the terms of higher order is negligible to those of lower order and the series may be truncated at some point and still be a good approximation of the expression.

There are different approaches to go from the discrete LBE to a continuous macroscopic equation. The most frequently applied one to obtain the Navier-Stokes equations is the Chapman-Enskog method [**?**], which will reproduce the compressible equations. An other method, often employed by M. Junk and his associates e.g. in [**?**], is a method based on regular asymptotic expansions, this is the method that will be utilised in this work and will in the case of Navier-Stokes reproduce the incompressible equations. A brief discussion of the differences between the Chapman-Enskog and the regular expansion approaches will be carried out at the end of this section.

The basic idea behind the analysis is to expand the distribution function f_i in some small parameter, ϵ. Also this parameter will be related to the spatial and time scales. The macroscopic limit is obtained by taking the taylor expansion of the discrete LBE and comparing terms of equal order in ϵ. Together with the fact that certain quantities is invariant under collisions, macroscopic differential equations is obtained. Now follows the part of the analysis which is common for the three equations, the more equation specific analysis is carried out in sections **??**, **??** and **??** respectively.

3.6.1 Motivation of the choice of expansion parameter

The expansion parameter should be a small dimensionless number. If the lattice is dense enough with respect to the characteristic length scale of the system, a suitable choice is the Knudsen number which is defined as the ratio of the mean free path, δ_x, and the characteristic length of the system under consideration, ℓ_0, i.e. $\epsilon = \delta_x/\ell_o$. To be able to perform the asymptotic analysis we must also relate the time scale to this parameter. From the fact that the lattice speed $c_s = \delta_x/\delta_t$ and by introducing a characteristic speed, $u_o = \ell_0/t_0$, we have

$$\epsilon = \frac{\delta_x}{\ell_0} = \frac{c_s}{u_0}\frac{\delta_t}{t_0} \tag{3.5}$$

It is now clear that what determines the relation between the timescale and the parameter ϵ is the ratio of the characteristic speed and the lattice speed which is usually referred to as the Mach number, Ma. In our particular case we will operate in the incompressible limit, i.e. $\mathrm{Ma} \ll 1$ and a suitable choice is a small number, thus $\mathrm{Ma} = \epsilon$ is chosen [?]. The discretisation of the space and time step is then

$$\delta_x'^2 = \delta_t' = \epsilon^2 \tag{3.6}$$

where the primes denote dimensionless variables. This particular scaling is usually referred to as diffusive scaling.

3.6.2 Expanding the LBE

The LBE, eq. (3.1), with dimensionless variables and the BGK collision operator reads:

$$f_i(\mathbf{x}' + \epsilon\mathbf{c}_i', t' + \epsilon^2) - f_i(\mathbf{x}', t') = -\omega\left[f_i(\mathbf{x}', t') - f_i^{(eq)}(\mathbf{x}', t')\right]. \tag{3.7}$$

The primes denoting dimensionless variables will, for readability reasons, from hereon be dropped. If nothing else is stated we always consider dimensionless variables.

To obtain a differential equation, the difference equation in eq. (3.7) is taylor expanded, which gives

$$\epsilon(\mathbf{c}_i\cdot\nabla f_i)+\epsilon^2(\partial_t f_i+(\mathbf{c}_i\cdot\nabla f_i)^2/2)+\epsilon^3(\partial_t(\mathbf{c}_i\cdot\nabla f_i)+(\mathbf{c}_i\cdot\nabla f_i)^3/6)+\mathcal{O}(\epsilon^4) = -\omega\left[f_i - f_i^{(eq)}\right] \tag{3.8}$$

Expanding also f_i and $f_i^{(eq)}$ in the parameter ϵ:

$$f_i = f_i^{(0)} + \epsilon f_i^{(1)} + \epsilon^2 f_i^{(2)} + \epsilon^3 f_i^{(3)} + \mathcal{O}(\epsilon^4) \tag{3.9}$$

$$f_i^{(eq)} = f_i^{(eq,0)} + \epsilon f_i^{(eq,1)} + \epsilon^2 f_i^{(eq,2)} + \epsilon^3 f_i^{(eq,3)} + \mathcal{O}(\epsilon^4) \tag{3.10}$$

and inserting these expressions into eq. (3.8) gives an equation with terms of varying orders of ϵ. Separating this equation in equations of common orders allows for an analysis of what happens at different scales of ϵ. For the four leading orders in ϵ we have:

$$\epsilon^0: \quad 0 = -\omega\left[f_i^{(0)} - f_i^{(eq,0)}\right], \tag{3.11}$$

$$\epsilon^1: \quad \mathbf{c}_i\cdot\nabla f_i^{(0)} = -\omega\left[f_i^{(1)} - f_i^{(eq,1)}\right], \tag{3.12}$$

$$\epsilon^2: \quad \mathbf{c}_i\cdot\nabla f_i^{(1)} + \partial_t f_i^{(0)} + (\mathbf{c}_i\cdot\nabla f_i^{(0)})^2/2 = -\omega\left[f_i^{(2)} - f_i^{(eq,2)}\right] \tag{3.13}$$

and

$$\epsilon^3: \quad \mathbf{c}_i \cdot \nabla f_i^{(2)} + \partial_t f_i^{(1)} + (\mathbf{c}_i \cdot \nabla f_i^{(1)})^2/2 + \partial_t(\mathbf{c}_i \cdot \nabla f_i^{(0)}) + (\mathbf{c}_i \cdot \nabla f_i^{(0)})^3/6 = -\omega \left[f_i^{(3)} - f_i^{(eq,3)} \right]. \tag{3.14}$$

The idea is now that for an equation of a particular order in ϵ, use collision invariants and eliminate unknown $f_i^{(n)}$:s by using equations of lower order in ϵ. This will in the end result in differential equations of macroscopic variables, given by moments of the f_i:s.

3.7 LBM for the Nernst-Planck equation

The method presented here is based on representing the Nernst-Planck equation, eq. (2.8), as an equation of advection-diffusion type. Considering the quantity:

$$\bar{\mathbf{u}} = \mathbf{u} - \frac{z q_e D}{k_B T} \nabla \psi \tag{3.15}$$

as an effective advective velocity, we have:

$$\frac{\partial \rho}{\partial t} + \nabla \cdot (\bar{\mathbf{u}} \rho - D \nabla \rho) = 0 \tag{3.16}$$

which is a mass conservation equation with fluxes from diffusion and from advection respectively. The letter c for denoting the charge concentration has in this section been replaced by the letter ρ for avoiding the risk of confusing it with the lattice velocities which traditionally are denoted by $\mathbf{c}_i$.

A collision operator of BGK type, eq. (3.2) will be used together with a D2Q9 lattice. The lattice-Boltzmann equation then reads:

$$f_i(\mathbf{x} + \mathbf{c}_i \delta_t, t + \delta_t) - f_i(\mathbf{x}, t) = -\omega \left[f_i(\mathbf{x}, t) - f_i^{(eq)}(\mathbf{x}, t) \right] \tag{3.17}$$

with $\{\mathbf{c}_i\}$ for the D2Q9 lattice as in eq. (**??**). The equilibrium function, $f_i^{(eq)}$, is chosen as [**?**]:

$$f_i^{(eq)} = w_i \rho \left(1 + \frac{\mathbf{c}_i \cdot \bar{\mathbf{u}}}{c_s^2} \right) \tag{3.18}$$

with the weights, w_i, as in eq. (3.3). The charge density and charge flux density is obtained by taking the zeroth and first moments of the distribution function respectively, i.e:

$$\rho = \sum_i f_i \tag{3.19}$$

and

$$\mathbf{j} = \sum_i f_i \mathbf{c}_i \tag{3.20}$$

The diffusion constant, D, is related to the relaxation parameter ω through

$$D = c_s^2 \left(\frac{1}{2} - \frac{1}{\omega} \right). \tag{3.21}$$

3.7.1 Asymptotic analysis

To motivate the appearance of the above suggested method for solving eq. (3.16) and for showing under what premises the method is valid, the macroscopic limit of the discrete scheme will now be analysed in an asymptotic manner.

From the expansion of f_i in eq. (3.9) and from eqs. (3.19) and (3.20) follow the expansions of the charge and flux density respectively as

$$\rho = \rho^{(0)} + \epsilon\rho^{(1)} + \epsilon^2\rho^{(2)} + \epsilon^3\rho^{(3)} + \mathcal{O}(\epsilon^4) \tag{3.22}$$

and

$$\mathbf{j} = \mathbf{j}^{(0)} + \epsilon\mathbf{j}^{(1)} + \epsilon^2\mathbf{j}^{(2)} + \epsilon^3\mathbf{j}^{(3)} + \mathcal{O}(\epsilon^4) \tag{3.23}$$

The advective velocity is also expanded as:

$$\bar{\mathbf{u}} = \bar{\mathbf{u}}^{(0)} + \epsilon\bar{\mathbf{u}}^{(1)} + \epsilon^2\bar{\mathbf{u}}^{(2)} + \epsilon^3\bar{\mathbf{u}}^{(3)} + \mathcal{O}(\epsilon^4) \tag{3.24}$$

By plugging these expansion into the equilibrium distribution eq. (3.18), the expansion in eq. (3.10) is obtained. The terms of order zero is used in the zeroth order equation of the LBE, eq. (3.11), which gives

$$f_i^{(0)} = w_i\rho^{(0)} \left(1 + \frac{\mathbf{c}_i \cdot \bar{\mathbf{u}}^{(0)}}{c_s^2} \right). \tag{3.25}$$

However, since we are only considering the low Mach limit, i.e. $|\bar{\mathbf{u}}| \sim \epsilon$, we will in this analysis assume that $\bar{\mathbf{u}}^{(0)} = 0$. And thus $\bar{\mathbf{u}}$ will be of order ϵ to leading order. It is possible to show [**?**] that if $\bar{\mathbf{u}}$ is initialised small it will also stay small if no major momentum sources are present, thus it is a question of proper initialisation if the assumption holds or not. Thus the expression for $f_i^{(0)}$ reduces to

$$f_i^{(0)} = w_i\rho^{(0)} \tag{3.26}$$

3.8 LBM for Navier-Stokes

3.8.1 Chapman-Enskog analysis

3.8.2 Forcing schemes

how to add a ”forcing” term in the method.

3.9 LBM for Poisson's equation

3.9.1 Chapman-Enskog

3.10 Algorithm/Scheme for solving the coupled equations

the iterative scheme used.

3.11 Boundary conditions

discussion and description of the boundary conditions

3.11.1 bounce back

accuracy, e.g. second order accurate if placed between node planes...

3.11.2 slip

3.11.3 he-zou, constant density/velocity

3.11.4 Maybe something on non-local boundary conditions

3.12 Physical units vs lattice units

how to interchange between them... etc...

3.13

4

A few notes on high performance computing

intro what is said below refer to computers of a certain architecture...

4.1 The pipeline

keep it full.

4.2 Locality

using the caches in a good way. some examples of its importance.

4.2.1 Locality and LBM

4.3 Parallelisation

shared memory, distributed memory...

data dependence, LBM good!

OpenMP/MPI

4.4 Maybe something about profiling

men kanske inte tillför något vettigt.

4.5 Choice of programming language

4.6 Some stats on the performance of the code...

Lattice updates/s

5

Model benchmarks

intro 2D

5.1 Poiseuille flow

First out for evaluating the LBM solver of the Navier-Stokes equations is the situation with Poiseuille flow. This is a classic example and one of the easiest situations were the NS equations are exact solvable. Consider a 2D channel of length l and width H. If the flow in this channel is driven by a constant force, e.g. a constant pressure drop, the velocity profile will adopt to a parabolic shape in the steady state situation. Here follows a brief derivation of the exact expression for the velocity profile.

Consider the (non-dimensional) Navier-Stokes eqs. (**??**) and (**??**) in 2D. Let x be the direction along the channel and y the direction across the channel. In the case of a pressure gradient in the x direction and no other external forces involved we deduce that the y component of the velocity is zero. Thus eq. (**??**) reduces to an equation for the x component of the velocity

$$\frac{\partial \mathrm{u_x}}{\partial t} - \mathrm{u_x}\frac{\partial \mathrm{u_x}}{\partial x} = \frac{1}{\mathrm{Re}}\frac{\partial^2 \mathrm{u_x}}{\partial y^2} - \frac{\partial \mathrm{P}}{\partial x}. \tag{5.1}$$

Under the assumption of a system in a steady state, i.e. $\partial \mathrm{u_x}/\partial t = 0$. Further if the flow is fully developed $\partial \mathrm{u_x}/\partial x = 0$, this also assures that (**??**) is fulfilled. We now have together with writing the constant pressure gradient as $\Delta \mathrm{P}/l$

$$\frac{\partial^2 \mathrm{u_x}}{\partial y^2} = \frac{\mathrm{Re}\,\Delta \mathrm{P}}{l}. \tag{5.2}$$

Solving this eq. with no slip boundary conditions, $\mathrm{u_x}(0) = \mathrm{u_x}(H) = 0$ gives an expression of the velocity profile

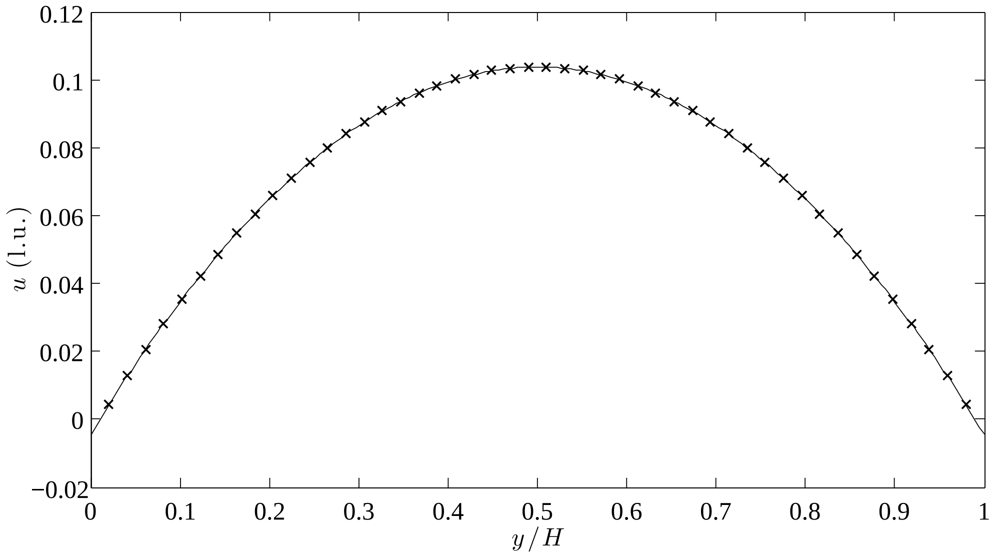

Figure 5.1: Obtained velocity profiles of Poiseuille flow ($\times$) compared to the analytical solution (solid line). A grid of 3$\times$50 nodes were used. As expected, there was no variation of the velocity field in the flow direction. The velocity is given in lattice units.

$$\mathrm{u_x}(y) = \frac{\mathrm{Re}\,\Delta\mathrm{P}}{2l} y(y - H). \tag{5.3}$$

The benchmark of the LBM solver of the NS equation described in section **??** was performed with a pressure gradient incorporated as a force. Other possibilities would be to drive the fluid by imposing fixed pressures/velocities at the inlet and outlet. In this case, with a driving force, periodic boundary conditions were imposed at the inlet and outlet. At the channel walls, the bounce-back boundary condition described in section **??** was imposed. The actual boundary will thus be located half a node-node distance into the fluid.

A grid with 50 nodes across the channel and 3 in the flow direction were used. The driving force was set to $\Delta\mathrm{P}/l = 1 \cdot 10^{-4}$ and the Reynolds number to $\mathrm{Re} = l_0 u_0/\nu$ where the viscosity is $\nu = 0.2778$ from eq. (**??**) with $\omega = 0.75$ and $l_0 = u_0 = 1$. The solution that was obtained after 20000 iterations is presented in fig. 5.1. The analytical solution, eq. (**??**), is plotted for comparison.

The agreement between computed and analytical solution is satisfying. With an RMS error of $9.271{\cdot}10^{-5}$ l.u. and maximum absolute error of $1.198{\cdot}10^{-4}$ l.u.. Note that the actual boundary is located half a node-node distance into the computational domain, this is due to the implementation of the bounce-back scheme, see section **??**.

5.2 Taylor-Green vortex

5.3 Helmholtz equation

The LB formulation for solving Poisson's equation as well as the implementation was tested by solving Helmholtz equation with a certain set of boundary conditions allowing for finding an analytical solution. The homogeneous Helmholtz equation reads:

$$\nabla\psi = \lambda^2\psi \tag{5.4}$$

where λ is a real parameter. The equation was solved for $\lambda = 2$ on the domain $(x, y) \in [0, 1] \times [0, 1]$ with the following Dirichlet boundary conditions:

$$\begin{aligned} &\psi(0, y) = -\psi(1, y) = \tfrac{\sinh\sqrt{\lambda^2+\pi^2}(1-y)}{\sinh\sqrt{\lambda^2+\pi^2}}, \\ &\psi(x, 0) = \cos\pi x, \;\; \psi(x, 1) = 0. \end{aligned} \tag{5.5}$$

The analytical solution to eq. (5.4) with the given boundary conditions is [?]:

$$\psi(x, y) = cos\pi x \frac{\sinh\sqrt{\lambda^2+\pi^2}(1-y)}{\sinh\sqrt{\lambda^2+\pi^2}}. \tag{5.6}$$

A grid of $n_x \times n_y = 65 \times 65$ nodes was used when computing the LBM solution. The computational domain was rescaled to the desired one by setting $\delta_x = 1/(n_x - 1) = 1/64$ and $\delta_t = \delta_x^2$. An other possibility would have been to rescale the parameter λ and have $\delta_x = \delta_t = 1$.

The boundary conditions in eq. (**??**) was implemented using the He/Zou approach described in section **??**. A bounce back approach with some momentum addition would also have been possible but was not chosen due to that the actual boundary location is not at the node location, but half a node-node distance into the computational domain. Also the bounce-back implementation is previously tested.

In fig. 5.2a, the obtained solution is presented together with the absolute error in fig. 5.2b. The agreement is satisfying, with an error which magnitude is about the same as in previous works [?]. The error takes on its maximum at the boundary of the domain, implying that the fulfilment of the boundary conditions is not complete.

5.4 Advection-Diffusion

Before the implementation of the Nernst-Planck part of the model is tested, a special case is considered, i.e. when the electrical potential in the domain is constant. This makes the source term including the electrical potential in eq. (**??**) vanish and we have to solve only for advection and diffusion.

Introducing characteristic scales for the concentration (C_0), advective velocity (u_0) and length (l_0) respectively, gives the non-dimensional advection-diffusion equation for incompressible flow:

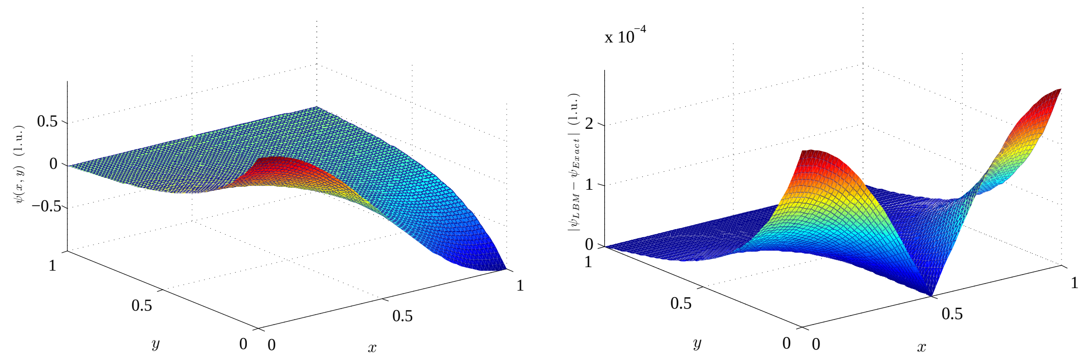

(a) Computed solution **(b)** Error

Figure 5.2: To the left, the obtained solution of the Helmholtz equation, eq. (5.4). To the right, the error.

$$\frac{\partial C}{\partial t} + \mathbf{u} \cdot \nabla C = \frac{D}{u_0 l_0} \nabla^2 C. \tag{5.7}$$

All variables in (5.7) are non-dimensional. The quantity $Pe = u_0 l_0 / D$ is often referred to as the Péclet number. It determines the relation between contributions to the dynamics from advection and diffusion respectively. For $Pe \gg 1$ the dynamics is dominated by advection and for $Pe \ll 1$ by diffusion.

The LB model described in section **??** was tested by studying the evolution in time and space of a point mass in one dimension. The analytical solution of eq. (5.7) in one dimension with initial conditions $C(x, t = 0) = \delta(x)$ on an infinite domain is:

$$C(x,t) = \sqrt{\frac{Pe}{4\pi t}} \exp\left(-\frac{(x - ut)^2 Pe}{4t} \right). \tag{5.8}$$

In the numerical computations the parameters $Pe = 10$ and $|\mathbf{u}| = 0.1$ were used. The domain consisted of 200 lattice nodes and three snapshots in time at $t = 100, 200, 300$ were compared to the analytical solution. The result is presented in fig. 5.3.

5.5 Nernst-Planck, a special case

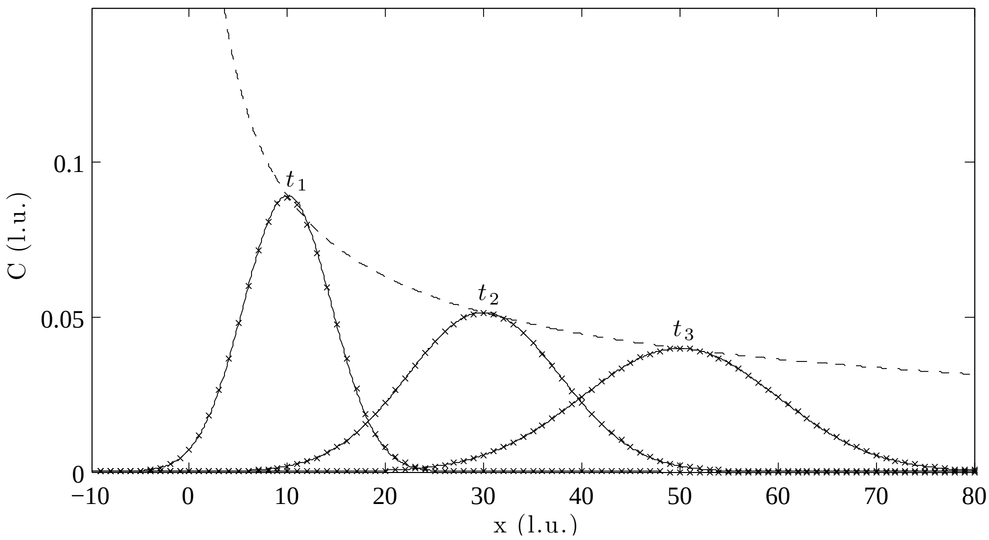

Figure 5.3: Obtained solutions ($\times$) of the advection-diffusion equation for a point mass evolving in time and space. Three different times ($t_n = 100n$) are compared to analytical solutions (solid). The Amplitude of the solutions as function of time has also been plotted (dashed). The advecting velocity, $u_0 = 0.1$ and the Peclet number, $Pe = 10$. All units are in lattice units.

6

Modelling of electrokinetic flow

6.1 Electric potential in 2D channel - PB

section in the channel, + debye-huckel comparision

6.1.1 It might be interesting to compare the two models Chai and Wang

6.2 Compare with Nernst-Planck

6.2.1 Potential

6.2.2 Charge distribution

6.3 Electroviscous effect

NP + PB differences?

6.4 Flow in array of charged squares

maybe other geometries as well?

6.5 3D?

only god knows...

7

Conclusions

And what do we conclude of this?